Drug Design, Development and Therapy

Dovepress
Taylor & Francis Group

Open Access Full Text Article

ORIGINAL RESEARCH

The Natural Compound Cornuside Protects Against Acute Liver Failure Induced by Lipopolysaccharide and D-Galactosamine

Lin Wang[1–3,*], Fenglian Yan[1,2,*], Ting Zhang[1], Zhaoming Zhong[1], Sen Yan[4], Xueyang Sun[1], Ziyu Liu[1], Yuqing Li[1], Junfeng Zhang[1,2], Chunxia Li[1,2], Bailiu Ya[1,2], Shang Chen[5], Huabao Xiong[1], Hui Zhang[1]

[1]Institute of Immunology and Molecular Medicine, Jining Medical University, Jining, Shandong, People's Republic of China; [2]Jining Key Laboratory of Immunology, Jining Medical University, Jining, Shandong, People's Republic of China; [3]Department of Immunology and National Key Laboratory of Immunology and Inflammation, Naval Medical University, Shanghai, People's Republic of China; [4]The First Clinical Medical College, Shandong University of Traditional Chinese Medicine, Jinan, Shandong, People's Republic of China; [5]Medical Research Center of Affiliated Hospital of Jining Medical University, Jining Medical University, Jining, Shandong, People's Republic of China

*These authors contributed equally to this work

Correspondence: Hui Zhang; Huabao Xiong, Institute of Immunology and Molecular Medicine, Jining Medical University, Jining, Shandong, People's Republic of China, Email zhanghuitjwh@hotmail.com; xionghbl@163.com

Purpose: Acute liver failure (ALF) is a life-threatening syndrome characterized by rapid hepatocyte injury, excessive inflammation, and oxidative stress. Cornuside, an iridoid glycoside derived from *Cornus officinalis* Sieb. et Zucc, has been reported to exert anti-inflammatory and antioxidant activities, but its role in ALF remains unclear. This study aimed to evaluate the preventive and therapeutic effects of cornuside in a lipopolysaccharide (LPS)/D-galactosamine (D-GalN)-induced mouse ALF model and to explore the underlying mechanisms.

Methods: ALF was induced in mice by intraperitoneal injection of LPS and D-GalN. Cornuside was administered via tail vein injection either 3 h before or 1 h after LPS/D-GalN administration to assess its preventive and post-injury therapeutic effects, respectively. Serum and liver tissues were harvested 12 h after LPS/D-GalN challenge for the assessment of liver injury, hepatocyte apoptosis, intrahepatic immune cell activation, inflammatory cytokine production, oxidative stress, and ferroptosis-associated markers.

Results: Cornuside administration after LPS/D-GalN challenge did not produce significant therapeutic protection against established ALF. In contrast, cornuside pretreatment markedly reduced serum alanine aminotransferase and aspartate aminotransferase levels, alleviated hepatic histopathological injury, and decreased hepatocyte apoptosis. Cornuside pretreatment also suppressed intrahepatic immune cell activation and reduced pro-inflammatory cytokine production. Moreover, cornuside attenuated oxidative stress, as indicated by reduced lipid peroxidation and enhanced antioxidant activity. Mechanistically, cornuside pretreatment modulated ferroptosis-associated signaling, including downregulation of ACSL4 and upregulation of xCT and Gpx4, suggesting that inhibition of ferroptosis may contribute to its hepatoprotective effects.

Conclusion: Cornuside provided significant preventive protection against LPS/D-GalN-induced ALF. This protection may be associated with inhibition of inflammation, oxidative stress, and ferroptosis-related ACSL4/xCT/Gpx4 signaling, suggesting cornuside as a potential preventive candidate for ALF.

Keywords: cornuside, acute liver failure, ferroptosis, oxidative stress, Traditional Chinese Medicine

Introduction

Acute liver failure (ALF), alternatively termed fulminant hepatic failure, is a life-threatening hepatic disorder characterized by rapid hepatocyte injury, extensive hepatic necrosis, severe deterioration of liver function, poor prognosis, and high mortality.[1] It has a multitude of etiologies and various clinical presentations that may involve multiple extrahepatic organ system. Despite recent advances in ALF treatment, liver transplantation remains the only effective treatment

https://doi.org/10.2147/DDDT.S601517
Received: 5 February 2026
Accepted: 25 May 2026
Published: 3 June 2026

Graphical Abstract

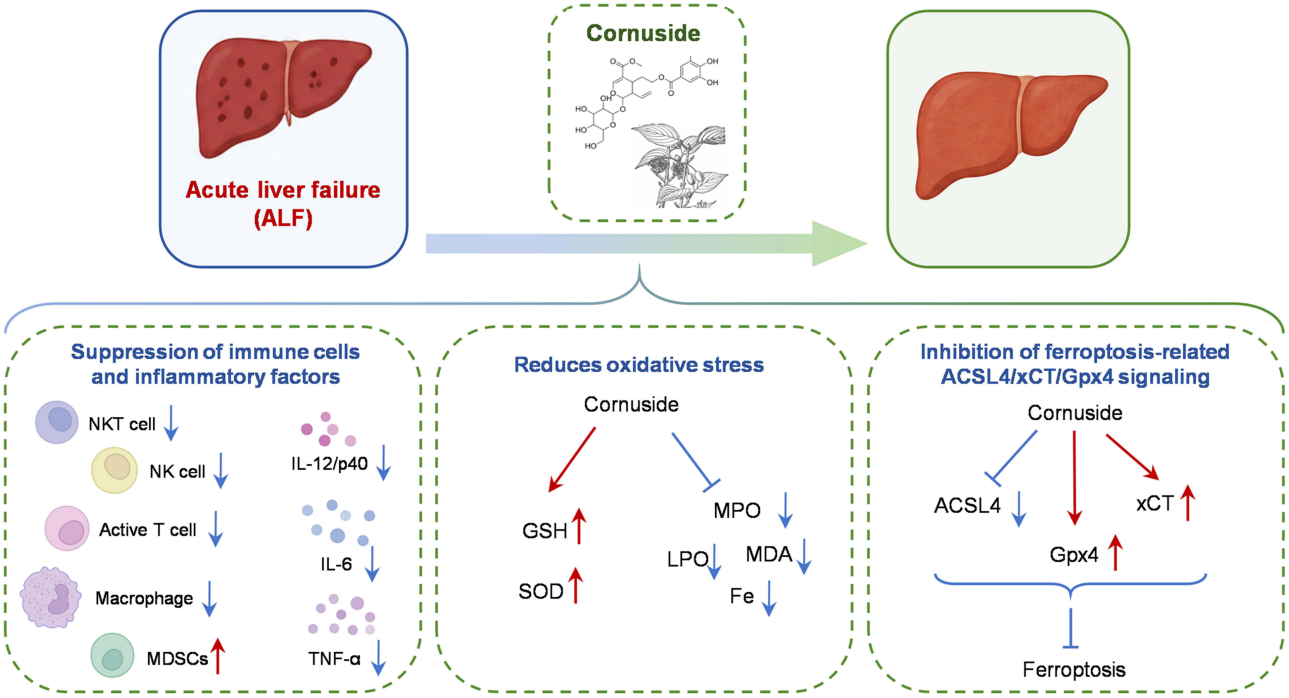

option. However, its clinical application is limited by donor shortage, transplant rejection, perioperative risks, and other complications, leaving many patients unable to receive effective treatment.[2] Thus, there is an urgent need to further elucidate the molecular mechanisms driving ALF pathogenesis and explore more efficient therapeutic strategies. Recent studies have increasingly emphasized that inflammatory cascade activation, oxidative stress, and ferroptosis-related hepatocyte injury collectively contribute to the initiation and progression of acute liver injury.[3–6] Beyond these injury-promoting mechanisms, hepatocyte-derived stress signals and nonparenchymal cell-mediated tissue remodeling have also been implicated in liver injury and repair, further underscoring the complexity of hepatic pathological responses.[7] These findings highlight the need for mechanism-based therapeutic interventions.

Lipopolysaccharide (LPS), also referred as endotoxin, is a key pathogenic component of the outer membrane of Gram-negative bacteria. It interacts with Toll-like receptor 4 (TLR4) to activate TLR4-dependent signaling in immune cells, particularly macrophages, initiating the secretion of pro-inflammatory cytokines—including interleukin-6 (IL-6), tumor necrosis factor-α (TNF-α), and IL-12/p40—and thereby mediating inflammatory responses.[8] LPS-induced inflammatory injury has also been linked to NF-κB activation, endothelial dysfunction, oxidative stress, and tissue damage in different experimental settings.[9] Meanwhile, D-galactosamine (D-GalN) potently suppresses hepatic RNA synthesis, thereby synergistically enhancing the liver's susceptibility to LPS-induced lethality and promoting hepatocyte apoptosis.[10] Accordingly, the LPS/D-GalN-induced ALF model is a well-established and reproducible experimental model that mimics key pathological features of ALF, including excessive inflammatory responses, rapid hepatocyte injury, oxidative stress, and cell death.[11] More importantly, these pathological events are highly consistent with the reported anti-inflammatory, antioxidant, immunomodulatory, and hepatoprotective activities of cornuside. Thus, this model is particularly suitable for evaluating whether cornuside can protect against ALF and for exploring its potential mechanisms of action. Recent pharmacological studies using this model have also supported its value for assessing candidate anti-inflammatory and hepatoprotective agents.[3]

Ferroptosis is a distinct iron-dependent form of regulated cell death characterized by iron overload, lipid peroxidation, and impairment of antioxidant defense. It differs from apoptosis and pyroptosis in its morphological, molecular, and biochemical

hallmarks.[12] Notably, different forms of regulated cell death may coexist or interact during liver injury and inflammatory diseases, suggesting that ferroptosis may contribute to hepatic damage together with other injury-related pathways.[4,13] The liver plays a central role in regulating systemic iron metabolism; therefore, disruption of hepatic iron homeostasis can aggravate oxidative injury, while persistent liver damage may further impair iron regulation, forming a vicious cycle of iron overload, lipid peroxidation and hepatocyte death.[14] Consistently, accumulating evidence has demonstrated that ferroptosis is involved in the pathogenesis of multiple liver diseases, including acute liver injury,[15] hemochromatosis,[16] alcohol-associated liver disease (ALD),[17] nonalcoholic steatohepatitis (NASH),[18] and hepatocellular carcinoma (HCC).[19,20] In addition, accumulating evidence has demonstrated that the dysregulation of ferroptosis-related signaling pathways, such as the CASTOR1/mTORC1/Gpx4 axis, is capable of inducing liver injury.[4] Consequently, targeting ferroptosis may represent a promising strategy for the prevention and treatment of ferroptosis-related liver injury and other hepatic disorders.

Natural compounds derived from traditional Chinese medicine (TCM) have attracted increasing attention as potential agents for the prevention and treatment of liver diseases. For instance, recent studies have shown that dihydroquercetin (DHQ)—a natural compound isolated from *Pinaceae* plants—alleviates ALF by suppressing ferroptosis.[21] Other natural compounds or biologically active agents have also been reported to mitigate liver injury by regulating oxidative stress, inflammatory signaling, gut barrier function, and cell-death-related pathways.[3,5,22,23] Cornuside (molecular formula: $C_{24}H_{30}O_{14}$), an iridoid glycoside naturally occurring in the fruits of *Cornus officinalis* Sieb. et Zucc, possesses a broad range of pharmacological activities. As a TCM-derived compound, it exerts hepatoprotective, neuroprotective, hypoglycemic, antioxidant, anti-inflammatory, and nephroprotective effects.[24] Previous studies has demonstrated the anti-inflammatory and antioxidant properties of cornuside in various inflammatory conditions, including sepsis, atopic dermatitis, carbon tetrachloride-induced acute liver injury, and encephalomyelitis.[25–28] In addition, our previous studies revealed that cornuside exhibits potent anti-inflammatory and antioxidant properties in concanavalin A (Con A)-induced autoimmune hepatitis.[29] However, whether cornuside protects against LPS/D-GalN-induced ALF, whether its effect depends on the timing of administration, and whether ferroptosis-associated signaling is involved remain unclear.

In this study, we aimed to evaluate the preventive and post-injury therapeutic effects of cornuside in an LPS/D-GalN-induced mouse model of ALF and to explore its potential mechanisms of action. Given the involvement of inflammation, oxidative stress, and ferroptosis-associated pathways in ALF, we investigated whether cornuside pretreatment could alleviate liver injury by modulating these pathological processes. Our findings provide experimental evidence that cornuside confers preventive hepatoprotection against ALF, at least in part, through suppression of inflammatory responses and oxidative stress, as well as regulation of ferroptosis-associated ACSL4/xCT/Gpx4 signaling.

Materials and Methods

Reagents

D-GalN and LPS were obtained from Sigma-Aldrich (St. Louis, MO, USA). Cornuside (Catalog No.: HY-N0631, purity: 99.95%) was acquired from MedChemExpress (Shanghai, China), with its chemical structure illustrated in Figure 1A. Assay kits for myeloperoxidase (MPO), tissue iron (Fe), malondialdehyde (MDA), lipid peroxidation (LPO), superoxide dismutase (SOD), and glutathione (GSH) were obtained from Nanjing Jiancheng Institute of Biological Engineering (Nanjing, China). Enzyme-linked immunosorbent assay (ELISA) kits targeting IL-6, TNF-α, and IL-12/p40, along with antibodies for flow cytometry, were sourced from BioLegend (San Diego, CA, USA). For Western blot analysis, antibodies against glutathione peroxidase 4 (Gpx4, Catalog No.: 52455S) were obtained from Cell Signaling Technology (Danvers, MA, USA). The Gpx4 antibody (Catalog No.: ab125066) for immunohistochemistry was purchased from Abcam (Cambridge, UK). Antibodies against xCT (Catalog No.: PT0398R) and Acyl-CoA synthetase long-chain family member 4 (ACSL4) (Catalog No.:PT0448R) for Western blot and immunohistochemistry was supplied by ImmunoWay (Beijing, China). The β-actin antibody (Catalog No.: AA128), RIPA Lysis Buffer (Catalog No.: P0013B) and Enhanced BCA Protein Assay Kit (Catalog No.: P0010) for Western blot were acquired from Beyotime (Shanghai, China). Reagents for quantitative reverse transcription polymerase chain reaction (qRT-PCR)—including HiScript III RT Super Mix (Catalog No.: R323) and AceQ qPCR SYBR Green Master Mix (Catalog No.: Q311)—were sourced from Vazyme (Nanjing, China).

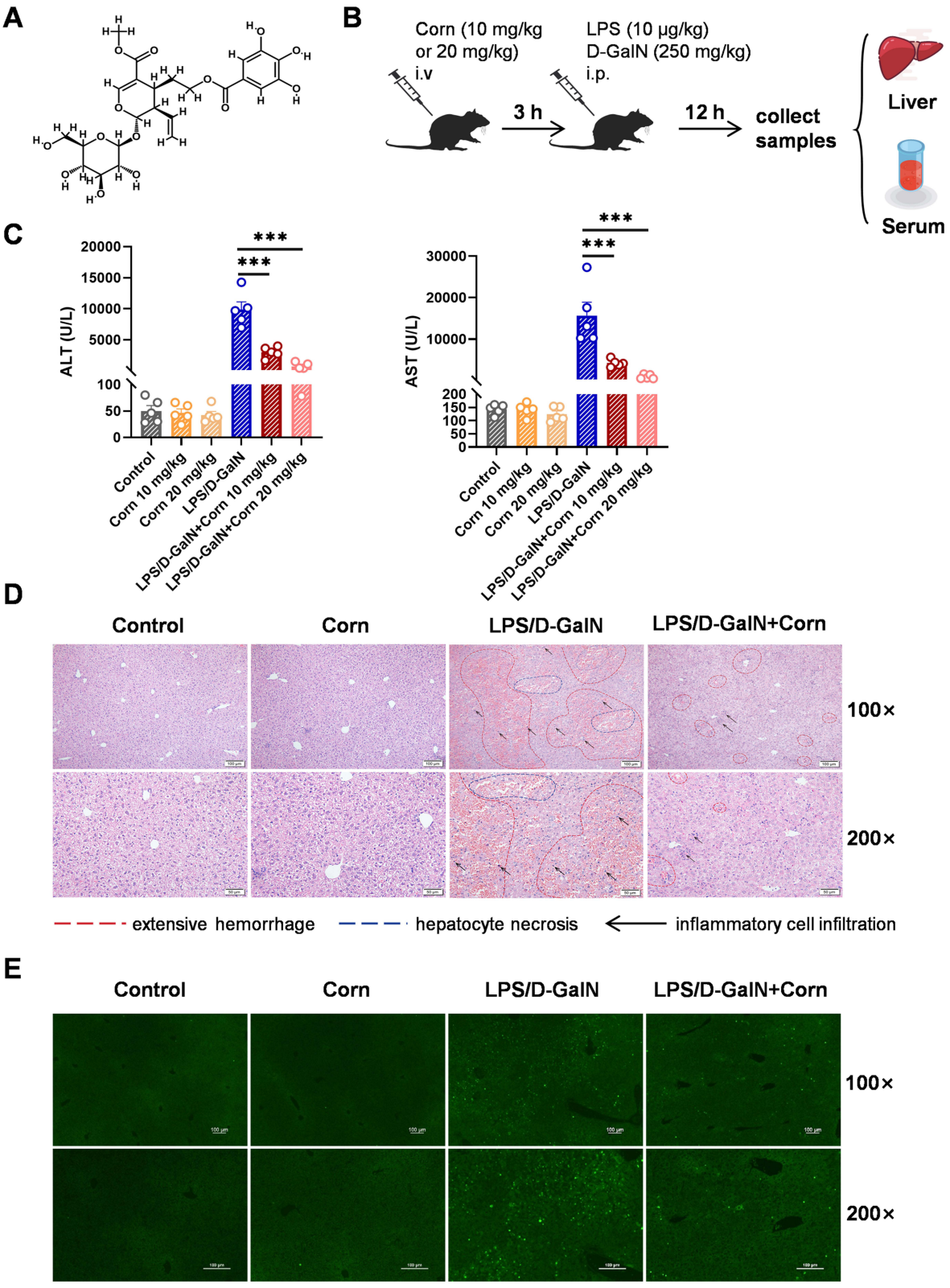

Figure 1 Pretreatment with cornuside mitigates LPS/D-GalN-induced ALF in mice. Mice were administered cornuside (10, 20 mg/kg body weight) via tail vein injection, followed by an intraperitoneal injection of LPS (10 μg/kg)/D-GalN (250 mg/kg) 3 h later. Serum and liver tissues were collected 12 h after LPS/D-GalN administration. (**A**) Chemical structure of cornuside. (**B**) Schematic diagram of the experimental design. (**C**) Serum alanine aminotransferase (ALT) and aspartate aminotransferase (AST) levels. (**D**) Liver sections were stained with hematoxylin and eosin (H&E). Representative histological images for each group are shown. Regions of extensive hemorrhage and hepatocyte necrosis are indicated by red dashed lines and blue dashed lines, respectively, while inflammatory cell infiltration is indicated by black arrows. Original magnifications: 100×, 200×. (**E**) One step TUNEL apoptosis assay of liver tissues, original magnifications: 100×, 200×. Data are presented as the mean ± standard error of the mean (SEM) (n = 5), ***$P < 0.001$.

https://doi.org/10.2147/DDDT.S601517

Network Pharmacological Analysis

Candidate targets with potential relevance to cornuside were retrieved from the PharmMapper Server. Subsequently, the gene symbols corresponding to these candidate targets were mapped to the UniProt database for standardized annotation. For the acquisition of disease-related targets, the Online Mendelian Inheritance in Man (OMIM, downloaded on August 18, 2025), DrugBank,[30] Therapeutic Target Database,[31] Disgenet[32] and GeneCards (version 5.25, last updated on July 16, 2025) databases were queried, with "acute liver failure" adopted as the search keyword. Overlapping genes (ie., common targets) between cornuside-related candidate targets and acute liver failure targets were analyzed and their relationships were visualized using the bioinformatics platform. To explore the biological functions and signaling pathways associated with these shared targets, enrichment analyses of the Kyoto Encyclopedia of Genes and Genomes (KEGG) pathways and Gene Ontology (GO) terms were conducted using Metascape. Additionally, a protein–protein interaction (PPI) network of the shared targets was constructed using the STRING database, with a confidence score threshold set at ≥ 0.4. The constructed PPI network was further visualized using the Cytoscape software (version Cytoscape_v3.8.2).

Mouse Model

Wild-type male C57BL/6 mice (6–8 weeks) were obtained from the Jinan Pengyue Animal Breeding Company (Jinan, China) and maintained in a specific pathogen-free (SPF) facility. All animal experiments were conducted in compliance with the Institutional Animal Welfare Guidelines and had been approved by the Animal Care and Use Committee of Jining Medical University (Approval No.: JNMC-2023-DW-131).

Cornuside, LPS, and D-GalN were dissolved in phosphate-buffered saline (PBS). ALF was induced by intraperitoneal injection of LPS (10 μg/kg) combined with D-GalN (250 mg/kg). Mice were randomly divided into the following groups: control, cornuside alone, LPS/D-GalN model, cornuside-pretreated LPS/D-GalN, and cornuside post-treated LPS/D-GalN groups. The control group received equivalent volumes of PBS, the cornuside-alone group received cornuside via tail vein injection, and the LPS/D-GalN model group received LPS/D-GalN without cornuside treatment. The tail vein injection route was selected based on our previous study[29] and to ensure rapid systemic delivery of cornuside in this acute injury model.

For the pretreatment protocol, cornuside was administered via tail vein injection at 10 or 20 mg/kg 3 h before LPS/D-GalN challenge. For the post-treatment protocol, cornuside was administered at 10 or 20 mg/kg 1 h after LPS/D-GalN challenge. Blood and liver samples were collected 12 h after LPS/D-GalN administration (Figure 1B).

Alanine Aminotransferase (ALT) and Aspartate Aminotransferase (AST) Assays

Animal blood samples were collected under anesthesia and allowed to clot at room temperature for 30 min. Samples were then centrifuged at 1900 × *g* for 15 min to obtain serum. ALT and AST levels were quantified using a Cobas 8000 modular analyzer (Roche Diagnostics, Basel, Switzerland).

Histopathological Analysis

Liver samples were fixed in 4% paraformaldehyde (Sigma-Aldrich), subjected to paraffin embedding, and sectioned into 5 μm-thick slices for hematoxylin and eosin (H&E) staining, as previously described.[33] To detect apoptosis, the terminal deoxynucleotidyl transferase-mediated dUTP nick-end labeling (TUNEL) assay was performed using a commercially available kit (Beyotime Biotechnology, Shanghai, China) to identify DNA strand breaks, following the manufacturer's recommended protocols. All histological evaluations were carried out using an Olympus microscope (Tokyo, Japan).

Immunohistochemistry (IHC) Staining

Paraffin-embedded liver tissue sections were dewaxed with xylene and rehydrated through a graded ethanol series. Subsequently, sections were treated with 3% hydrogen peroxide (H_2O_2) for 10 min to quench endogenous peroxidase activity. Nonspecific binding was blocked by incubating sections with 1% bovine serum albumin (BSA) at room temperature for 30 min. Sections were then incubated with primary antibodies at 4 °C overnight. The following day, sections were incubated with biotin-labeled secondary antibodies at room temperature for 1 h, followed by incubation

with a streptavidin-HRP complex (1:200 dilution) at room temperature for 30 min. Sections were subsequently incubated with 3,3'-diaminobenzidine (DAB) substrate for 5 min to induce color development and counterstained with hematoxylin for 1 min. Finally, the sections were mounted with coverslips and examined under a microscope (Olympus).

Assessment of SOD, MDA, MPO, LPO, GSH and Fe

Malondialdehyde (MDA), lipid peroxidation (LPO), myeloperoxidase (MPO), iron, and glutathione (GSH) levels, together with superoxide dismutase (SOD) activity, were measured in liver tissues using commercial assay kits. In HepG2 cells, MDA and LPO levels and SOD activity were also quantified using corresponding assay kits. Liver samples were homogenized in saline (10% w/v) and cultured HepG2 cells were lysed by ultrasonication. All samples were processed according to the manufacturers' protocols.

Determining Serum Cytokine Concentrations

Concentrations of inflammatory cytokines (IL-6, TNF-α, and IL-12/p40) in mouse serum were determined using specific mouse ELISA kits (BioLegend, USA). All assays, including appropriate standard curves and control samples, were conducted in accordance with the manufacturer's recommended procedures.

RNA Isolation and qRT-PCR

Following the manufacturer's guidelines, RNAiso Plus reagent was used to extract total RNA from mouse liver tissue. Next, 1 μg of the isolated total RNA was reverse-transcribed into complementary DNA (cDNA). Quantitative real-time PCR (qPCR) analysis was conducted on a Light Cycler 480 system with AceQ qPCR SYBR Green Master Mix. All specific primers employed are provided in Table 1. To assess alterations in mRNA expression relative to the control group, the $2^{-\Delta\Delta CT}$ method was used, with glyceraldehyde-3-phosphate dehydrogenase (GAPDH) serving as the internal reference gene.

Isolation of Hepatic Mononuclear Cells (HMNCs)

First, the mouse liver was perfused with 20 mL of phosphate-buffered saline (PBS). After the liver was excised, it was homogenized through a 200-gauge stainless steel mesh using PBS, followed by centrifugation at 1000 × *g* for 10 minutes. To eliminate residual tissue fragments, cell pellets was resuspended in 50 mL PBS, and then centrifuged at 20 × *g* for 5 min. The resulting supernatant was collected and further centrifuged at 700 × *g* for 8 min. The cell pellets were then resuspended in 40% percoll, carefully layered onto 70% percoll, and centrifuged at 700 × *g* for 30 min. Mononuclear cells were harvested from the density gradient interface, washed twice with PBS, and finally resuspended in RPMI-1640 medium at 2×10^6 cells/mL for subsequent flow cytometric analysis.

Table 1 Gene-Specific Primers

	Forward (5′–3′)	Reverse (5′–3′)
IFN-γ	ATGAACGCTACACACTGCATC	CCATCCTTTTGCCAGTTCCTC
TNF-α	GCCACCACGCTCTTCTGTCT	GGTCTGGGCCATAGAACTGATG
IL-6	CCAGAAACCGCTATGAAGTTCCT	CACCAGCATCAGTCCCAAGA
IL-1β	GAAATGCCACCTTTTGACAGTG	TGGATGCTCTCATCAGGACAG
IL-12	AGACATGGAGTCATAGGCTCTG	CCATTTTCCTTCTTGTGGAGCA
iNOS	CTGCAGCACTTGGATCAGGAACCTG	GGAGTAGCCTGTGTGCACCTGGAA
GAPDH	AACGACCCCTTCATTGAC	TCCACGACATACTCAGCAC

Flow Cytometry

The isolated HMNCs were washed twice with PBS and resuspended to obtain a single-cell suspension. The cells were then incubated with the appropriate fluorochrome-conjugated antibodies at 4 °C in the dark for 30 min. After two additional washes with PBS, the cells were subjected to analyze on a BD FACSVerse flow cytometer (BD Biosciences, USA) in accordance with the manufacturer's instructions.

Cell Culture

HepG2 cells were obtained from the Cell Bank of the Chinese Academy of Sciences (Shanghai, China) and cultured in Dulbecco's Modified Eagle Medium (DMEM; Gibco, USA) supplemented with 10% fetal bovine serum (FBS; Gibco, USA). The cells were maintained at 37 °C in a humidified incubator with 5% CO_2.

Cell Viability Assay

HepG2 cells were seeded into 96-well plates at a density of 5×10^4 cells/well and exposed to varying concentrations of cornuside (18.75–300 μM) and D-GalN (5–50 mM) separately for 24 h. Cell viability was evaluated using the CellTiter-Lumi Luminescent Cell Viability Assay Kit (Beyotime Biotechnology, China) in accordance with the manufacturer's instructions. In a subsequent experiment, HepG2 cells were first pretreated with cornuside (50, 100, 150 μM) for 3 h, followed by incubation with a pre-determined optimal concentration of D-GalN (20 mM, which induces a 50% reduction in cell viability) for an additional 24 h, after which cell viability was determined.

Western Blot Analysis

Liver tissues and HepG2 cells collected in vitro were lysed in RIPA lysis buffer supplemented with protease inhibitors. Protein concentrations were quantified using an enhanced BCA assay kit (Beijing Bio-Tenmai Biotechnology, China). Equal amounts of protein were separated by SDS-PAGE and transferred onto 0.45 μm PVDF membranes (Millipore, USA). After blocking with 3% BSA, membranes were incubated overnight with primary antibodies (1:1000). Following three washes with Tris-buffered saline with Tween-20 (TBST), horseradish peroxidase (HRP)-conjugated secondary antibodies were applied for 2 h at 25 °C. Protein bands were detected using an enhanced chemiluminescence system (Millipore, USA), with β-actin serving as the loading control.

Statistical Analysis

Statistical analyses were performed with GraphPad Prism 8.0 (San Diego, CA, USA). All data are presented as mean ± standard error of the mean (SEM). Group differences were evaluated by Student's *t*-test or one-way analysis of variance (ANOVA), with statistical significance indicated as $*P < 0.05$, $**P < 0.01$, and $***P < 0.001$.

Results

Cornuside Protects Against LPS/D-GalN-Induced ALF

Building on our previous study demonstrating the anti-inflammatory efficacy of cornuside in concanavalin A (Con A)-induced acute liver injury,[29] we further investigated its protective potential against LPS/D-GalN-induced ALF. Serum ALT and AST, two well-established clinical indicators of hepatocellular injury,[34] were measured to evaluate liver damage. To clarify the influence of administration timing, cornuside was administered either 3 h before or 1 h after LPS/D-GalN injection. Post-treatment with cornuside at 10 or 20 mg/kg failed to significantly reduce serum ALT and AST levels compared with the LPS/D-GalN model group (Supplementary Figure 1), indicating that cornuside did not exert obvious therapeutic effects after ALF induction. By contrast, cornuside pretreatment reduced the LPS/D-GalN-induced elevation of serum ALT and AST levels, with the 20 mg/kg dosage showing a more pronounced protective effect (Figure 1C). Therefore, 20 mg/kg cornuside pretreatment was used in all subsequent experiments.

Histological analysis by hematoxylin and eosin (H&E) staining revealed that LPS/D-GalN-induced ALF was characterized by extensive hemorrhage, hepatocyte necrosis, and massive inflammatory cell infiltration (Figure 1D). These pathological alterations were markedly alleviated in mice pretreated with 20 mg/kg cornuside. We next performed

TUNEL staining to evaluate hepatocyte apoptosis in liver tissue sections. Consistent with the histological findings, cornuside pretreatment substantially attenuated LPS/D-GalN-induced hepatocyte apoptosis (Figure 1E). Collectively, these findings demonstrate that cornuside protects against LPS/D-GalN-induced ALF in mice when administered before injury induction, supporting its preventive rather than post-injury therapeutic role in this model.

Network Pharmacology Analysis Provides Mechanistic Clues for the Protective Effects of Cornuside in ALF

To obtain preliminary mechanistic clues and to guide subsequent experimental validation, we first performed a network pharmacology analysis to identify potential targets and biological processes associated with the protective effects of cornuside in ALF. Using PharmMapper with a normal fit threshold of ≥ 0.6, we identified 149 potential target candidates for cornuside. In parallel, 1712 genes associated with acute liver failure were retrieved from OMIM, DrugBank, the Therapeutic Target Database, DisGeNET, and GeneCards. Intersection analysis identified 45 overlapping genes as common targets of both cornuside and acute liver failure (Figure 2A). Protein–protein interaction (PPI) network analysis of these shared targets identified seven hub genes: albumin (ALB), epidermal growth factor receptor (EGFR), caspase-3 (CASP3), estrogen receptor 1 (ESR1), peroxisome proliferator-activated receptor gamma (PPARG), SRC, and glycogen synthase kinase 3 beta (GSK3B) (Figure 2B). KEGG pathway enrichment analysis showed that these overlapping genes were distributed across 135 signaling pathways, which were further classified into 14 functional clusters, with the most representative pathways illustrated in Figure 2C. In particular, CASP3, EGFR, GSK3B, SRC, and PPARG—were significantly enriched in the MAPK signaling pathway, while CASP3 was also associated with the apoptosis pathway. GO biological process analysis indicated that ESR1, CASP3, PPARG, and SRC were involved in regulating inflammatory responses. In addition, GSK3B, SRC, and PPARG participated in apoptotic signaling, and both CASP3 and SRC were enriched in oxidative stress–related pathways (Figure 2D). These results suggest that the protective effects of cornuside against acute liver failure may mediated through the modulation of these processes which provided a mechanistic rationale for our subsequent experimental analyses. Since inflammation, immune cell activation, hepatocyte apoptosis, oxidative stress, and ferroptosis are closely interconnected during ALF progression, we next examined whether cornuside pretreatment could regulate these pathological events in LPS/D-GalN-induced ALF. Accordingly, serum inflammatory cytokines, hepatic immune cell activation, oxidative stress markers, and ferroptosis-associated signaling molecules were evaluated in the following experiments.

Cornuside Inhibits Inflammatory Cytokine Release in ALF Induced by LPS/D-GalN

Inflammation is a key contributor to the pathogenesis of acute liver failure.[35] To further elucidate the role of cornuside in suppressing LPS/D-GalN-induced inflammatory responses, we measured the serum protein levels of IL-6, IL-12/p40, and TNF-α by ELISA, as well as the hepatic mRNA expression of inflammatory mediators by qRT-PCR. The ELISA results showed that cornuside markedly reduced the serum levels of IL-6, IL-12/p40, and TNF-α (Figure 3A). Consistently, cornuside also downregulated the hepatic mRNA expression of *IL-6, IL-12, TNF-α, inducible nitric oxide synthase (iNOS), interferon-γ (IFN-γ)*, and *IL-1β* (Figure 3B). These results are consistent with the network pharmacology-based prediction, suggesting that cornuside inhibits the inflammatory response induced by LPS/D-GalN.

Cornuside Modulates Immune Cell Responses in LPS/D-GalN-Induced ALF

Multiple studies have demonstrated that immune cells play a pivotal role in the pathogenesis of acute liver failure (ALF), while cornuside has been shown to effectively regulate immune cell activity in inflammatory diseases.[29,36] In this study, we investigated the immunomodulatory effects of cornuside on immune cells in LPS/D-GalN-induced ALF. Flow cytometry analysis showed that cornuside pretreatment had no significant effect on the proportion of hepatic T cells ($CD3^+NK1.1^-$) (Figure 4A and B), but reduced the proportions of hepatic NK cells ($CD3^-NK1.1^+$) and NKT cells ($CD3^+NK1.1^+$) (Figure 4C and D). Further analysis of immune cell activation showed that cornuside pretreatment markedly suppressed the activation of T cells (Figure 4E and F) and NKT cells (Figure 4G), but had no significant effect on NK cell activation (Figure 4H). Subsequent analysis of T-cell subsets showed that cornuside pretreatment did not significantly

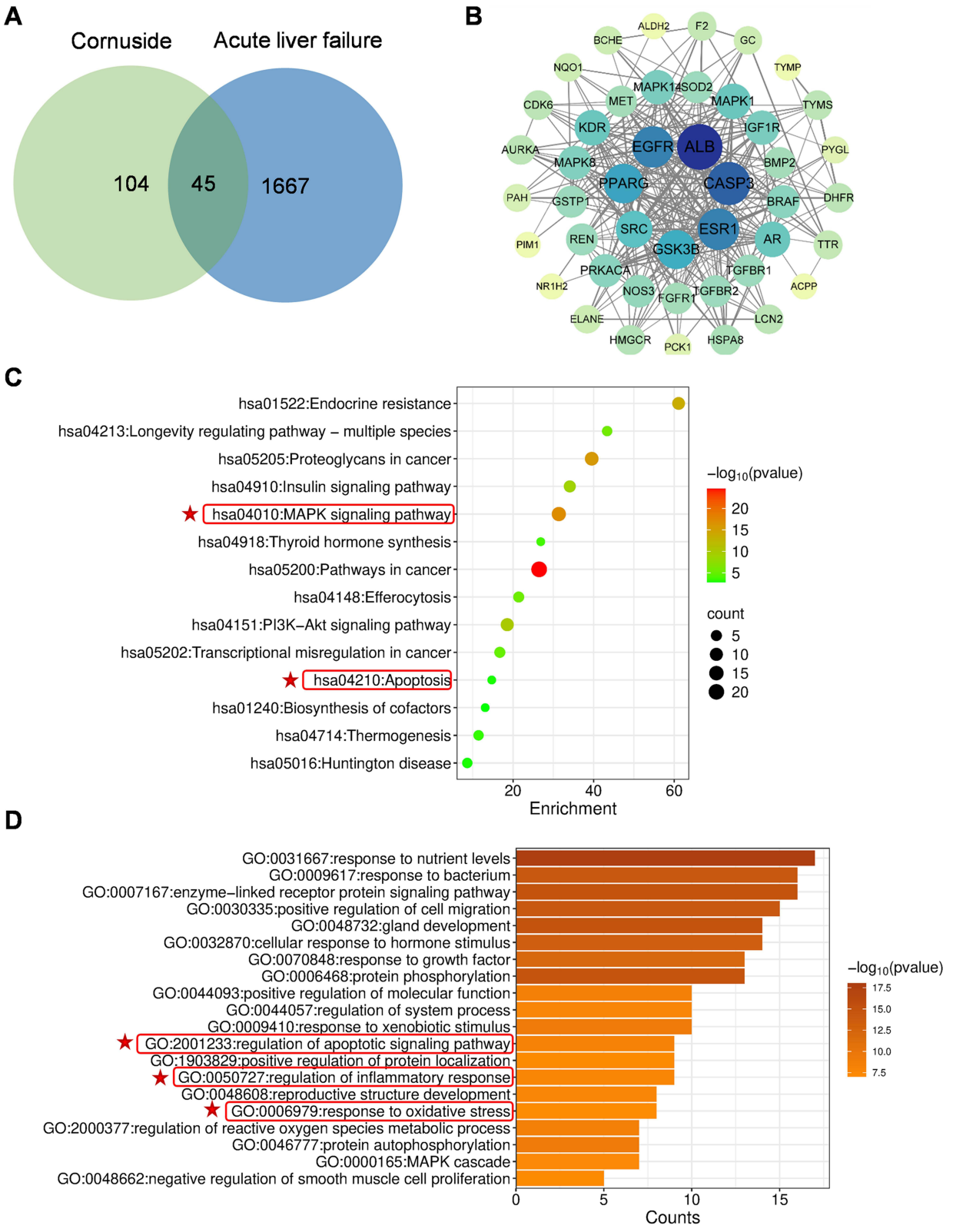

Figure 2 Network pharmacological analysis of cornuside. (**A**) Shared target genes of cornuside and ALF. (**B**) Protein–protein interaction network (PPI) of the shared target genes. Circle represents a target gene, and each line represents a protein–protein interaction. Circle size and color indicate the degree value of each node: larger and darker blue circles represent highly connected hub genes, whereas smaller light green or yellow circles represent genes with lower connectivity. (**C**) Kyoto Encyclopedia of Genes and Genomes (KEGG) analysis of the shared genes. (**D**) Gene Ontology (GO) biological process enrichment analysis of the shared genes. Relevant terms were highlighted with red frames and stars.

https://doi.org/10.2147/DDDT.S601517

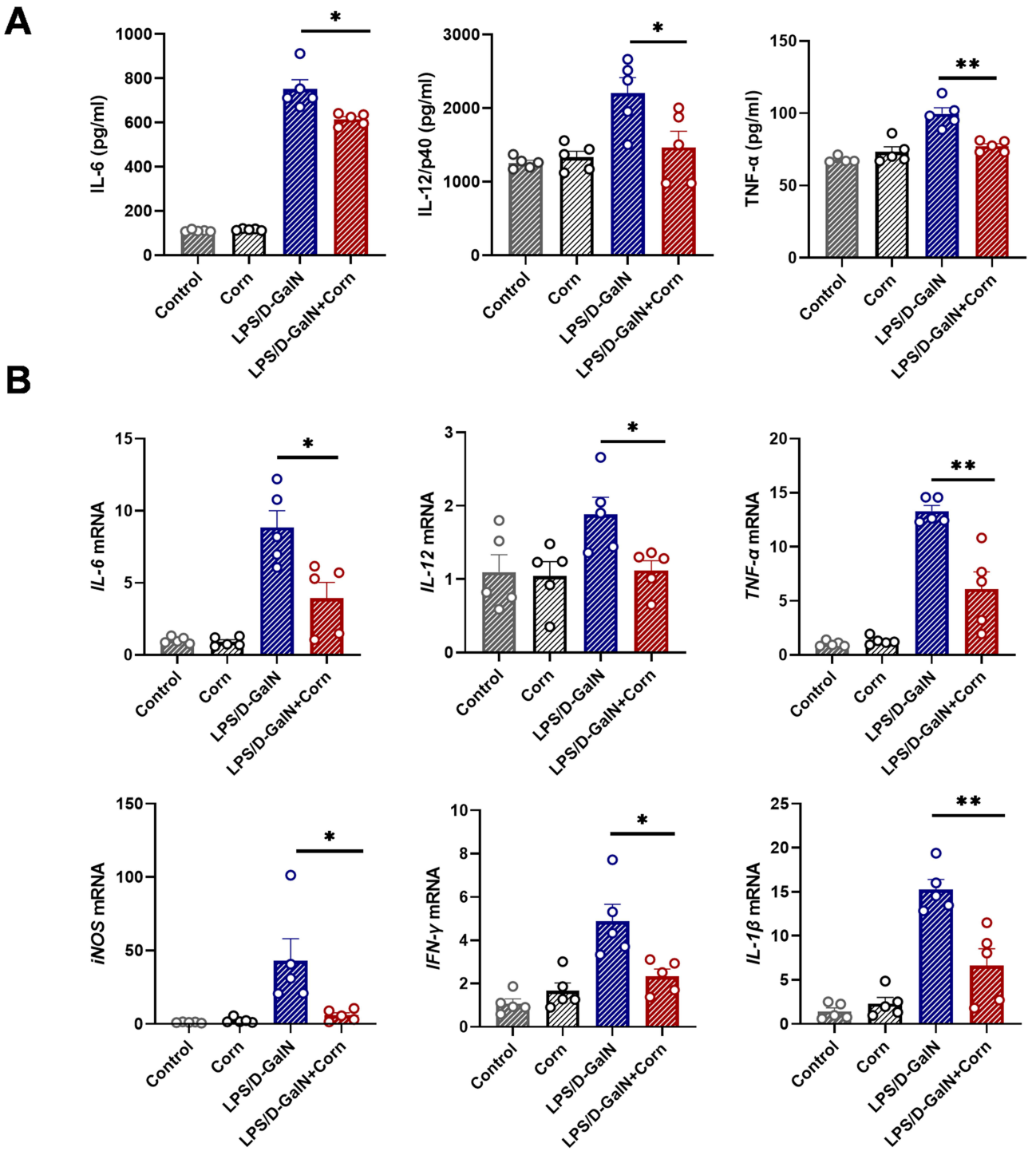

Figure 3 Cornuside reduces inflammatory cytokine levels in LPS/D-GalN-induced acute liver failure. Mice were treated as shown in Figure 1B. Serum and liver tissues were collected 12 h after LPS/D-GalN injection. (**A**) Serum concentrations of interleukin-6 (IL-6), IL-12/p40, and tumor necrosis factor-α (TNF-α). (**B**) Hepatic mRNA expression levels of *IL-6, IL-12, TNF-α, iNOS, IFN-γ*, and *IL-1β*. Data are presented as the mean ± SEM (n = 5). **P* < 0.05, ***P* < 0.01.

alter the proportions of $CD4^+$ T cells or $CD8^+$ T cells (Figure 5A–C), whereas it markedly inhibited the activation of these subsets (Figure 5D–F). Notably, in the ALF mouse model, cornuside treatment increased the proportion of myeloid-derived suppressor cells (MDSCs) among liver immune cells (Figure 6A and B) and reduced macrophage infiltration and activation (Figure 6C). Collectively, these findings suggest that cornuside mainly modulates hepatic immune responses

https://doi.org/10.2147/DDDT.S601517

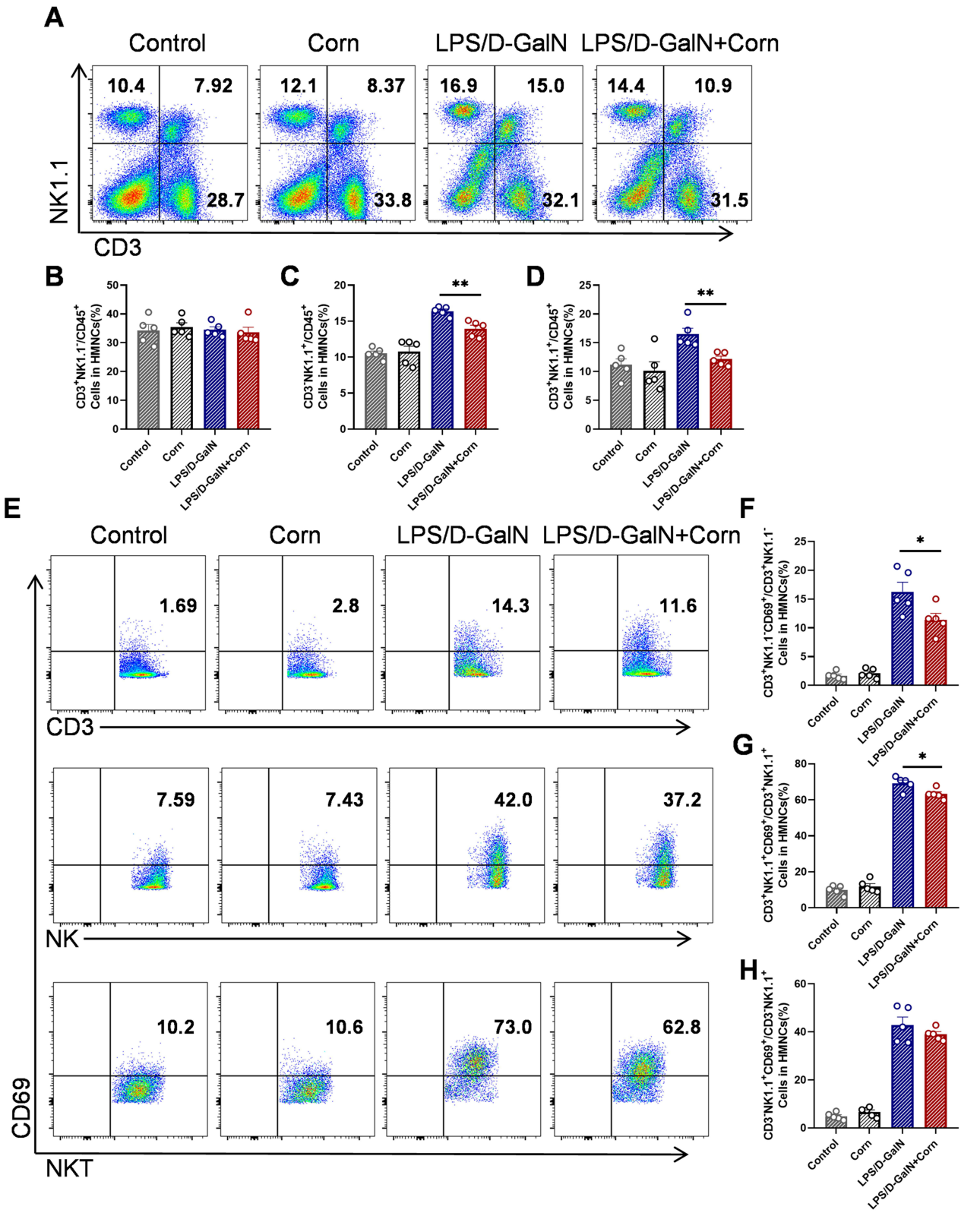

Figure 4 Cornuside inhibits the activation of T and NKT cells in the liver. Mice were treated as shown in Figure 1B. Liver tissues were collected 12 h after LPS/D-GalN injection. (**A**) Proportions of T ($CD3^+NK1.1^-$), NK ($CD3^-NK1.1^+$) and NKT ($CD3^+NK1.1^+$) cells. Statistical analysis of flow cytometry data for T ($CD3^+NK1.1^-$) (**B**), NK ($CD3^-NK1.1^+$) (**C**), NKT ($CD3^+NK1.1^+$) (**D**) cells. (**E**) Proportions of active T ($CD3^+NK1.1^-CD69^+$), NK ($CD3^-NK1.1^+CD69^+$) and NKT ($CD3^+NK1.1^+CD69^+$) cells. Statistical analysis of flow cytometry data for active T ($CD3^+NK1.1^-CD69^+$) (**F**), NKT ($CD3^+NK1.1^+CD69^+$) (**G**) and NK ($CD3^-NK1.1^+CD69^+$) (**H**) cells. Data are presented as the mean ± SEM (n = 5). $^*P < 0.05$, $^{**}P < 0.01$.

https://doi.org/10.2147/DDDT.S601517

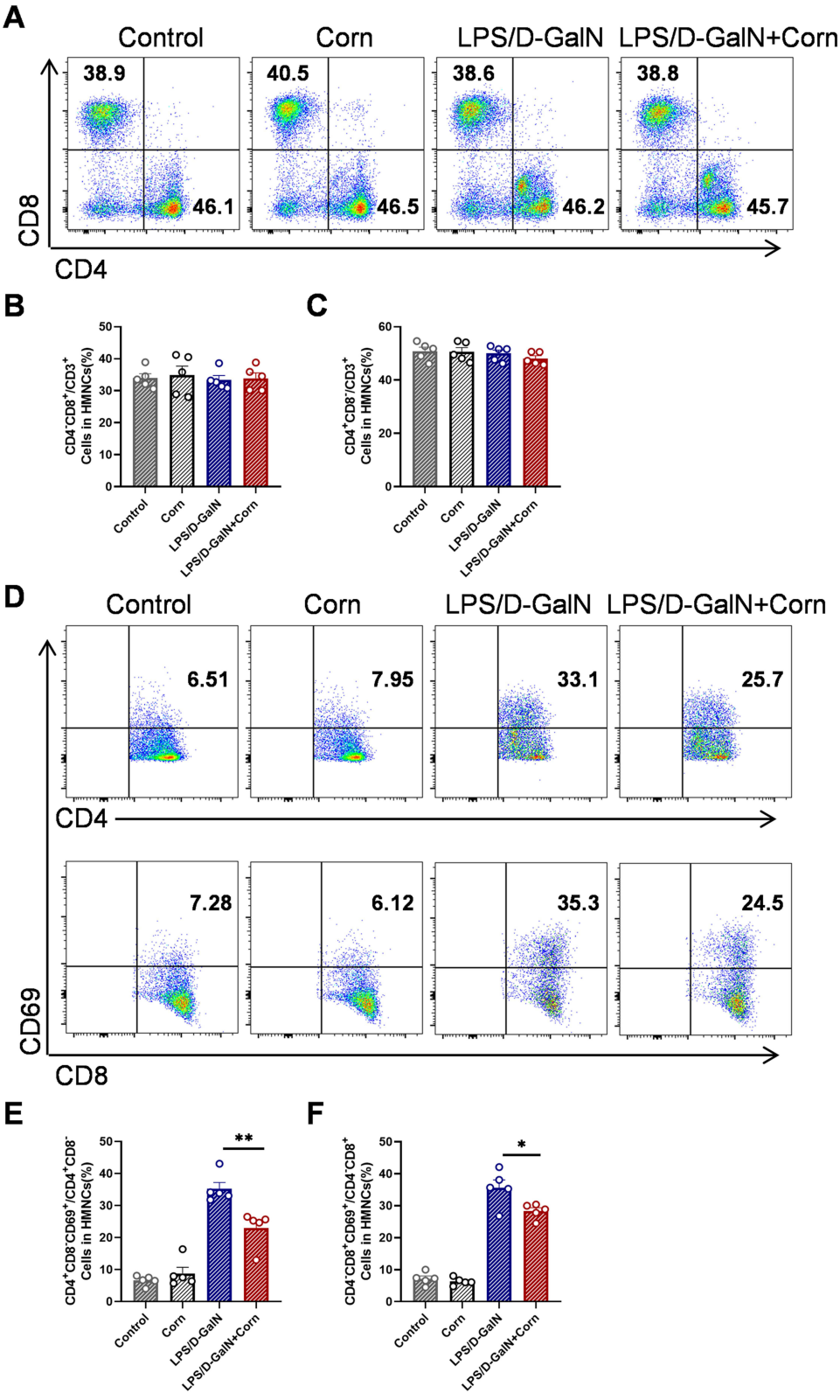

Figure 5 Cornuside inhibits the activation of $CD4^+$T and $CD8^+$T in the liver. Mice were treated as shown in Figure 1B. Liver tissues were collected 12 h after LPS/D-GalN injection. (**A**) Proportions of $CD4^+$T ($CD3^+CD4^+$) and $CD8^+$T ($CD3^+CD8^+$). Statistical analysis of flow cytometry data for $CD8^+$T ($CD3^+CD8^+$) (**B**), $CD4^+$T ($CD3^+CD4^+$) (**C**). (**D**) Proportions of active $CD4^+$T ($CD3^+CD4^+CD69^+$) cells and active $CD8^+$ T ($CD3^+CD8^+CD69^+$) cells. Statistical analysis of flow cytometry data for active $CD4^+$T ($CD3^+CD4^+CD69^+$) cells (**E**) and active $CD8^+$ T ($CD3^+CD8^+CD69^+$) cells (**F**). Data are presented as the mean ± SEM (n = 5). $^*P < 0.05$, $^{**}P < 0.01$.

https://doi.org/10.2147/DDDT.S601517

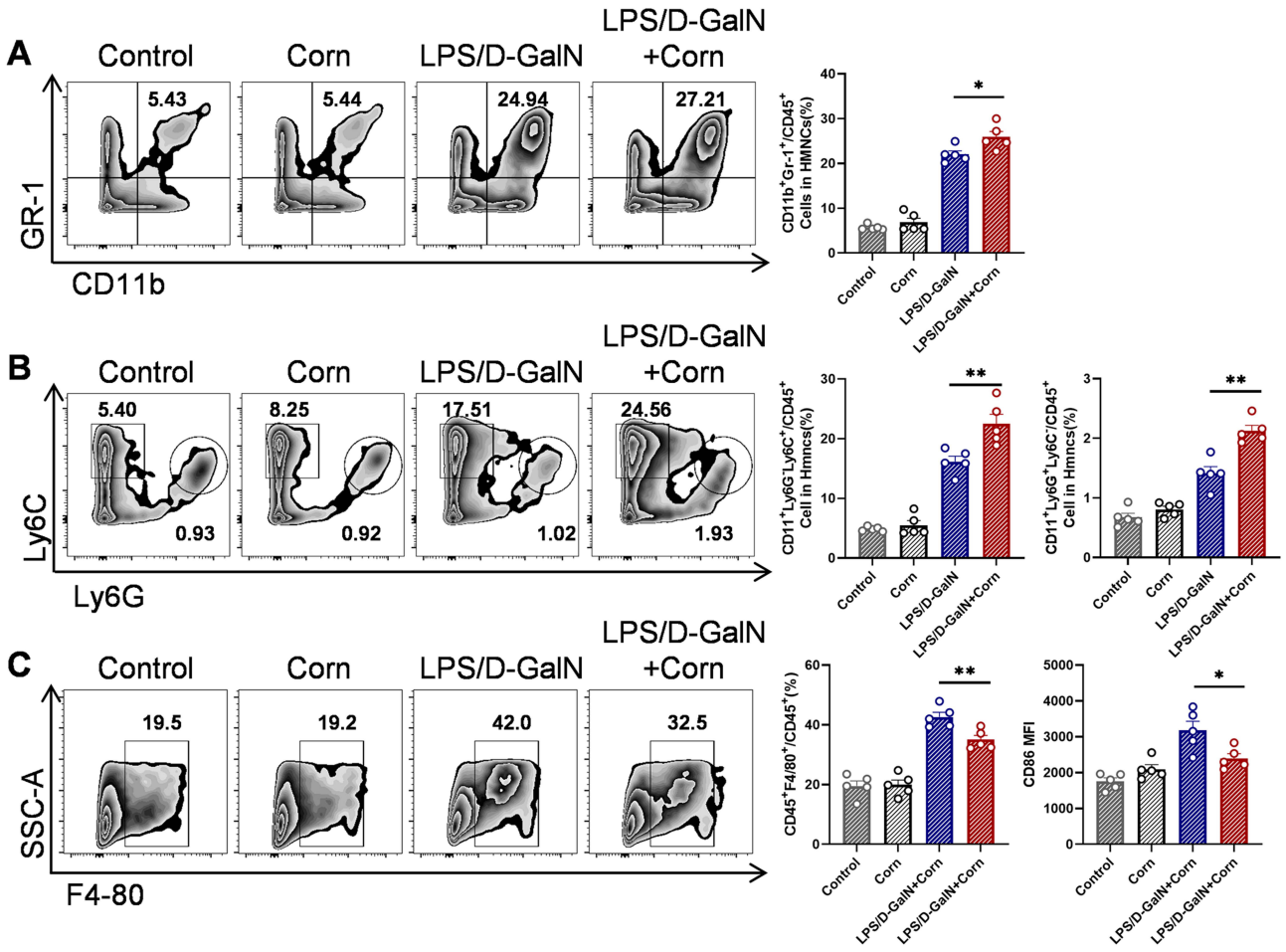

Figure 6 Cornuside modulates hepatic MDSCs populations and reduces macrophage infiltration. Mice were treated as shown in Figure 1B. Liver tissues were collected 12 h after LPS/D-GalN injection. (**A**) Percentage of $CD11b^+Gr\text{-}1^+$ MDSCs. (**B**) Percentage of $CD11b^+Ly6C^{int}Ly6G^{high}$ granulocytic MDSCs and $CD11b^+Ly6C^{high}Ly6G^{low}$ monocytic MDSCs. (**C**) Proportion of macrophages ($F4/80^+CD11b^+$) and CD86 MFI. Data are presented as the mean ± SEM (n = 5). $^*P < 0.05$, $^{**}P < 0.01$.

by suppressing T-cell and NKT-cell activation, reducing NK and NKT cell accumulation, increasing MDSCs proportions, and inhibiting macrophage infiltration and activation.

Cornuside Reduces Oxidative Stress in LPS/D-GalN-Induced ALF

Given the critical role of oxidative stress in the pathogenesis of ALF,[37] we evaluated the effects of cornuside on LPS/D-GalN-induced hepatic oxidative stress. As illustrated in Figure 7, pretreatment with cornuside led to a significant reduction in MDA levels (Figure 7A) and lipid peroxidation (LPO) levels (Figure 7B), indicating attenuated lipid peroxidation and oxidative membrane damage. Moreover, MPO activity, a well-established indicator of neutrophil infiltration and oxidative injury,[35] was substantially reduced in cornuside-treated mice (Figure 7C). Meanwhile, cornuside pretreatment decreased hepatic Fe accumulation (Figure 7D) and restored endogenous antioxidant defenses, as evidenced by increased SOD activity (Figure 7E) and GSH levels (Figure 7F). Since iron accumulation, lipid peroxidation, and GSH depletion are closely associated with ferroptosis, these findings suggest that cornuside may alleviate oxidative stress-related and ferroptosis-associated biochemical alterations in LPS/D-GalN-induced ALF.[38] To further determine whether cornuside directly protects hepatocytes against oxidative injury, we performed in vitro experiments using D-GalN-challenged HepG2 cells. Consistent with the in vivo findings, cornuside significantly reduced intracellular MDA (Figure 7G) and LPO levels (Figure 7H), while simultaneously enhancing SOD activity (Figure 7I). These results indicate that cornuside attenuates oxidative stress both in liver tissues and hepatocyte-like cells, supporting the network pharmacology prediction that oxidative stress-related biological processes may be involved in the hepatoprotective effects of cornuside.

https://doi.org/10.2147/DDDT.S601517

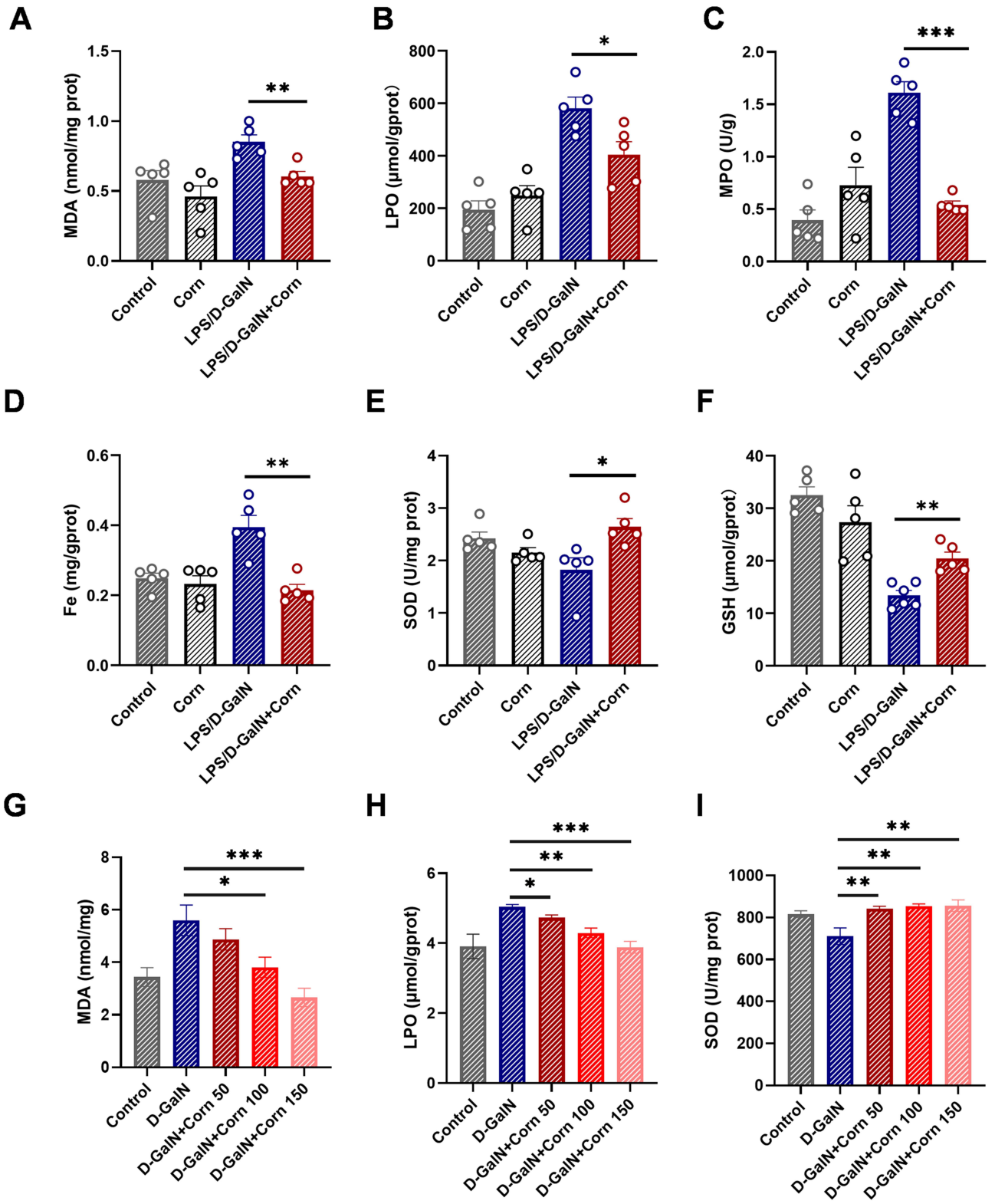

Figure 7 Cornuside reduces oxidative stress in LPS/D-GalN-treated livers and D-GalN-treated HepG2 cells. Mice were described as shown in Figure 1B. Liver tissues were collected 12 h after LPS/D-GalN injection and homogenized to determine malondialdehyde (MDA) levels (**A**), lipid peroxidation (LPO) levels (**B**), myeloperoxidase (MPO) levels (**C**), iron content (**D**), superoxide dismutase (SOD) activity (**E**), and glutathione (GSH) levels (**F**). To further evaluate the effects of cornuside on D-GalN-induced oxidative stress in vitro, HepG2 cells were used to measure MDA levels (**G**), LPO levels (**H**), and SOD activity (**I**). Data are presented as the mean ± SEM (n = 5). *$P < 0.05$, **$P < 0.01$, ***$P < 0.001$.

https://doi.org/10.2147/DDDT.S601517

Cornuside Alleviates Acute Liver Failure by Inhibiting Ferroptosis via the ACSL4/xCT/Gpx4 Pathway

Recent studies confirmed the occurrence of ferroptosis in ALF and its pivotal role in LPS/D-GalN-induced hepatic injury.[36,37] Given the well-established crosstalk between oxidative stress and ferroptosis, and based on the observed changes in ferroptosis-related biochemical indicators, including Fe, GSH, LPO, and MDA, we further investigated whether cornuside pretreatment modulated ferroptosis-associated changes in liver tissues after LPS/D-GalN challenge. We focused on ACSL4, xCT, and Gpx4 because these molecules are closely involved in lipid peroxidation susceptibility, cystine/glutathione metabolism, and lipid peroxide detoxification, respectively.[39] Notably, while LPS/D-GalN challenge increased ACSL4 accumulation in mouse liver tissues as shown by immunohistochemistry, cornuside treatment markedly reduced ACSL4 levels and concurrently elevated xCT and Gpx4 expression (Figure 8A and B). Western blot analysis further showed that cornuside pretreatment upregulated xCT, and Gpx4 expression and downregulated ACSL4 expression compared with the LPS/D-GalN model group (Figure 8C–F). To further support the in vivo findings, we performed in vitro experiments using HepG2 cells. We first evaluated the cytotoxicity of cornuside. As shown in Figure 9A, cornuside exhibited no significant effect on HepG2 cell viability at concentrations of ≤150 μM, suggesting no obvious cytotoxicity under the present in vitro experimental conditions. Based on this result, non-cytotoxic concentrations of cornuside were used in subsequent experiments. D-GalN stimulation markedly reduced HepG2 cell viability, whereas cornuside treatment significantly restored cell viability in D-GalN-challenged cells (Figure 9B and C). We next examined whether this protective effect was associated with ferroptosis-related alterations. Cornuside reduced intracellular Fe accumulation in D-GalN-challenged HepG2 cells (Figure 9D). In addition, Western blot analysis demonstrated that cornuside upregulated the protein expression of xCT and Gpx4 (Figure 9E and F). These results indicate that regulation of ferroptosis-related xCT/Gpx4 signaling may contribute to the preventive hepatoprotective effects of cornuside in LPS/D-GalN-induced ALF.

Discussion

ALF is a life-threatening syndrome characterized by rapid and extensive hepatocyte death, dramatically elevated aminotransferase levels, coagulopathy, and encephalopathy.[35] Although liver transplantation has significantly reduced the mortality of ALF, its clinical application is limited by donor shortage, postoperative complications, infection, immune rejection, and high medical burden.[35,40] Therefore, further elucidation of the mechanisms underlying ALF and identification of safe and effective preventive or early-intervention strategies remain important.

Natural products and traditional Chinese medicine-derived compounds have attracted increasing attention in the prevention and treatment of liver diseases because of their multi-target pharmacological properties.[41–44] Several plant-derived active compounds have been reported to alleviate experimental ALF by regulating inflammation, oxidative stress, apoptosis, mitochondrial injury, and ferroptosis-related pathways.[21,36,45,46] For example, sarmentosin attenuates acetaminophen-induced ALF by reducing reactive oxygen species production through regulation of USP17 and Nrf2 signaling.[46] The Yi-Qi-Jian-Pi formula effectively ameliorated pathological damage in LPS/D-GalN-induced ALF.[45] Dihydroquercetin has also been shown to alleviate ALF by regulating the SIRT1/p53 signaling axis and inhibiting both ferroptosis and mitochondrial apoptosis pathways.[21] These studies suggest that natural products may provide useful pharmacological tools for targeting multiple pathological processes involved in ALF.

Cornuside, an iridoid glycoside derived from *Cornus officinalis* Sieb. et Zucc, has been reported to possess anti-inflammatory and antioxidant activities. Our previous study also demonstrated that cornuside attenuated concanavalin A-induced autoimmune hepatitis.[29] However, whether cornuside protects against LPS/D-GalN-induced ALF and which mechanisms are involved had not been fully clarified. The present study demonstrates that cornuside provides significant preventive protection against LPS/D-GalN-induced ALF when administered before injury induction. Notably, cornuside administration after LPS/D-GalN challenge did not produce obvious therapeutic protection under the current experimental conditions, indicating that protective role of cornuside observed in this study should be interpreted mainly as a preventive or early-intervention effect rather than as a therapeutic effect against established ALF.

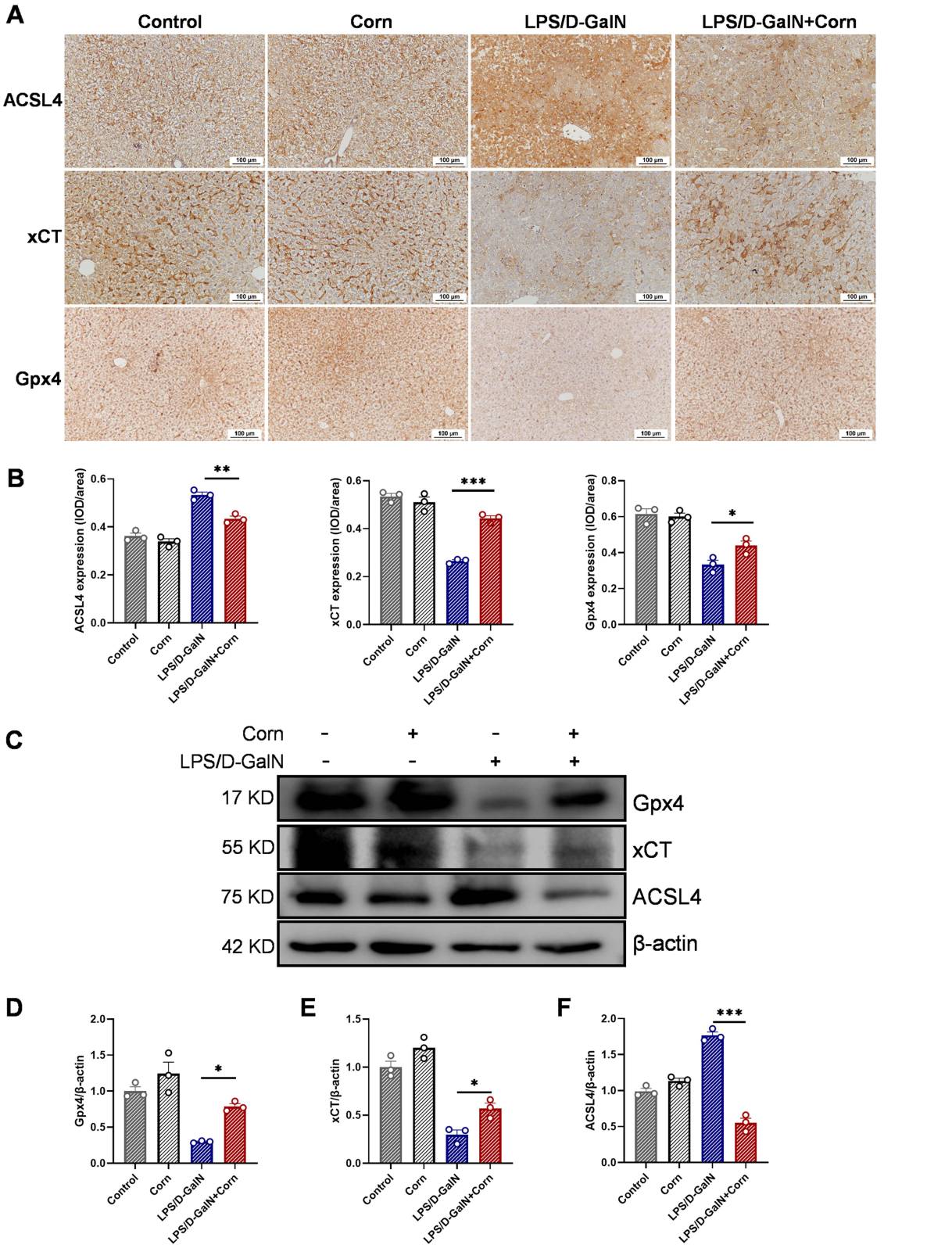

Figure 8 Cornuside mitigates ferroptosis triggered by LPS/D-GalN. Mice were treated as shown in Figure 1B. (**A**) Immunohistochemical staining of ACSL4, xCT and Gpx4 in liver tissue sections. Original magnification: 200×. Representative histological images for each group are shown. (**B**) Quantitative analysis of the immunohistochemical staining for ACSL4, xCT, and Gpx4. (**C**) Western blot analysis of Gpx4, xCT, and ACSL4 in liver tissues. Statistical analysis of Gpx4 (**D**), xCT (**E**), and ACSL4 (**F**) expression levels in Western blot. Data are presented as the mean ± SEM (n = 3). **P* < 0.05, ***P* < 0.01, ****P* < 0.001.

https://doi.org/10.2147/DDDT.S601517

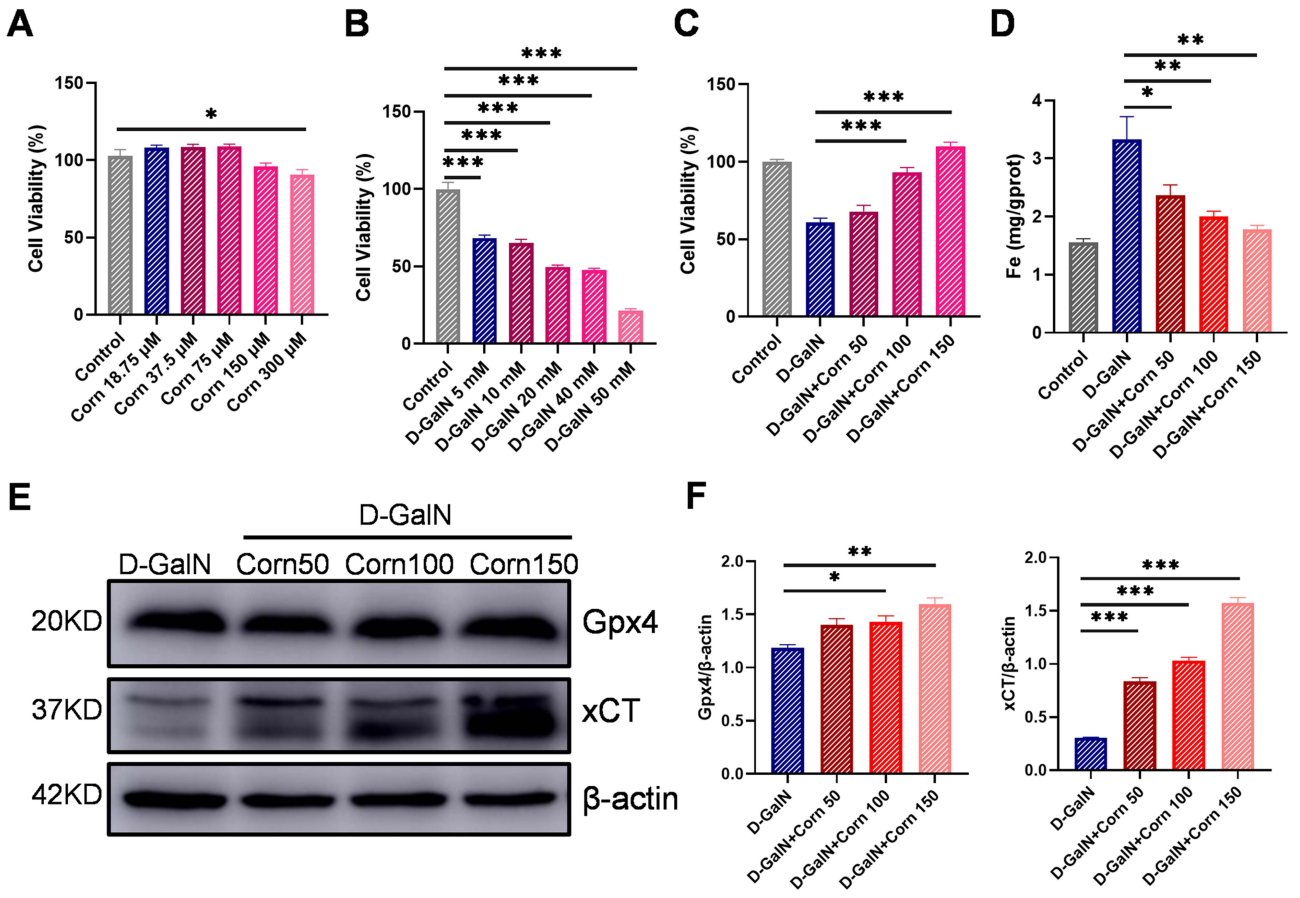

Figure 9 Cornuside alleviates ferroptosis triggered by D-GalN in vitro. (**A**) The effect of cornuside on the cell viability of HepG2 cells. (**B**) The effect of D-GalN on the cell viability of HepG2 cells. (**C**) Cornuside can alleviate the death of HepG2 cells induced by D-GalN. (**D**) Cornuside reduces the accumulation of iron (Fe) levels induced by D-GalN. (**E**) Western blot analysis of key proteins of ferroptosis (Gpx4 and xCT). (**F**) Statistical analysis of Gpx4 and xCT expression levels. Data are presented as the mean ± SEM (n = 3). **P* < 0.05, ***P* < 0.01, ****P* < 0.001.

Next, network pharmacology analysis was used as an exploratory approach to generate mechanistic clues. The enrichment of shared cornuside-ALF targets in inflammation-, apoptosis-, and oxidative stress-related processes provided the rationale for subsequent experimental validation, including cytokine detection, immune cell profiling, TUNEL staining, oxidative stress assays, and ferroptosis-associated analysis.

The pathogenesis and progression of ALF involve complex pathological mechanisms. Multiple etiological factors (including viruses, alcohol, and drugs) can directly induce hepatocyte apoptosis, necrosis, and other forms of regulated cell death, leading to primary liver injury.[35] In addition, injured hepatocytes release damage-associated molecular patterns, which activate Kupffer cells and recruited immune cells. These immune cells produce large amounts of pro-inflammatory cytokines, such as TNF-α, IL-6, and IL-12/p40, and promote the infiltration of neutrophils and monocytes into liver tissues. Persistent activation of these inflammatory cascades can amplify hepatocyte injury and contribute to secondary liver damage.[35,47] Thus, simultaneous regulation of hepatocyte death and inflammatory responses may represent an effective strategy for attenuating ALF progression.

Consistent with this concept, our results showed that cornuside pretreatment significantly reduced serum ALT and AST levels and alleviated histopathological liver damage in LPS/D-GalN-treated mice. H&E staining showed that cornuside pretreatment attenuated hepatic hemorrhage, hepatocyte necrosis, and inflammatory cell infiltration. TUNEL staining further demonstrated that cornuside reduced LPS/D-GalN-induced hepatocyte apoptosis. In parallel, flow cytometry analysis showed that cornuside suppressed intrahepatic immune cell activation, and cytokine analysis confirmed that cornuside decreased pro-inflammatory cytokine production in both serum and liver tissues. These findings

https://doi.org/10.2147/DDDT.S601517

suggest that cornuside protects against ALF, at least in part, by reducing hepatocyte apoptosis and limiting excessive inflammatory responses.

Oxidative stress is another key contributor to LPS/D-GalN-induced hepatotoxicity. Excessive production of reactive oxygen species and impaired antioxidant defense can promote lipid peroxidation, mitochondrial dysfunction, inflammatory amplification, and hepatocyte death.[38,48] In the present study, cornuside pretreatment significantly reduced hepatic MDA and LPO levels, indicating attenuation of lipid peroxidation and oxidative membrane damage. Cornuside also decreased MPO activity, suggesting reduced neutrophil-associated oxidative injury. In addition, cornuside restored endogenous antioxidant defense capacity, as reflected by increased SOD activity and GSH levels. These in vivo findings were further supported by the in vitro experiments in D-GalN-challenged HepG2 cells. Together, these results indicate that cornuside consistently attenuates oxidative stress under both in vivo and in vitro ALF-related conditions.

Oxidative stress is closely linked to ferroptosis, an iron-dependent form of regulated cell death characterized by iron accumulation, lipid peroxidation, and disruption of cellular redox homeostasis. Recent studies have identified ferroptosis as an important mechanism contributing to acute and chronic liver diseases.[49] Because lipid peroxidation, GSH depletion, and iron accumulation are central biochemical features of ferroptosis,[50] the observed effects of cornuside on hepatic Fe levels, lipid peroxidation, SOD activity, and GSH content suggest that cornuside may also modulate ferroptosis-associated alterations during ALF. However, these biochemical changes alone are not sufficient to fully establish ferroptosis inhibition; therefore, we further examined key ferroptosis-related markers in liver tissues and HepG2 cells.

The ACSL4/xCT/Gpx4 axis is a central regulatory network involved in ferroptosis by coordinating lipid metabolism, cystine uptake, GSH synthesis, and lipid peroxide detoxification.[39] ACSL4, a key mediator of the canonical ferroptotic pathway, regulates ferroptosis by catalyzing the acylation of polyunsaturated fatty acids (PUFAs). Overexpression of ACSL4 promotes the generation of lipid peroxidation substrates while simultaneously suppressing Gpx4 activity, thereby exacerbating redox system imbalance and accelerating ferroptosis progression.[20] In the present study, LPS/D-GalN challenge increased hepatic ACSL4 expression, whereas cornuside pretreatment reduced ACSL4 expression in liver tissues, suggesting decreased ferroptosis susceptibility. In contrast, xCT, the functional subunit of system Xc−, promotes cystine uptake and supports GSH synthesis, thereby maintaining Gpx4 activity and cellular antioxidant capacity.[51] Our immunohistochemical and Western blot results showed that cornuside increased xCT expression in liver tissues and HepG2 cells. As the key enzyme responsible for reducing lipid hydroperoxides, Gpx4 catalyzes the reduction of lipid peroxides to nontoxic lipid alcohols using GSH as its substrate, thereby terminating lipid peroxidation cascades and negatively regulating ferroptosis.[52] Consistently, Gpx4 expression was increased in the cornuside-pretreated group compared with the LPS/D-GalN model group. Taken together, these results suggest that cornuside pretreatment modulates ferroptosis-associated ACSL4/xCT/Gpx4 signaling, which may contribute to its preventive hepatoprotective effects against LPS/D-GalN-induced ALF.

It should be noted that this study has several limitations. First, cornuside showed significant protective effects only when administered before LPS/D-GalN challenge, whereas post-injury administration did not produce obvious therapeutic efficacy under the current experimental conditions. Therefore, the present findings mainly support the preventive or early-intervention potential of cornuside rather than its therapeutic effect against established ALF. Second, although our data suggest the involvement of ferroptosis-associated ACSL4/xCT/Gpx4 signaling, further studies using specific ferroptosis modulators, genetic approaches, or rescue experiments are needed to confirm the causal role of ferroptosis. Third, the current safety evaluation was preliminary. Future studies should systematically assess the long-term toxicity, pharmacokinetics, bioavailability, optimal dosing regimen, and safety profile of cornuside to support its further translational development.

Conclusion

In summary, this study demonstrates that cornuside pretreatment protects against LPS/D-GalN-induced ALF. The hepatoprotective effects of cornuside may be associated with suppressing excessive inflammatory responses, reducing oxidative stress, and modulating ferroptosis-associated ACSL4/xCT/Gpx4 signaling (Figure 10). These findings provide experimental evidence supporting cornuside as a potential preventive candidate for ALF, although additional mechanistic, pharmacokinetic, safety, and therapeutic-window studies are required before clinical translation.

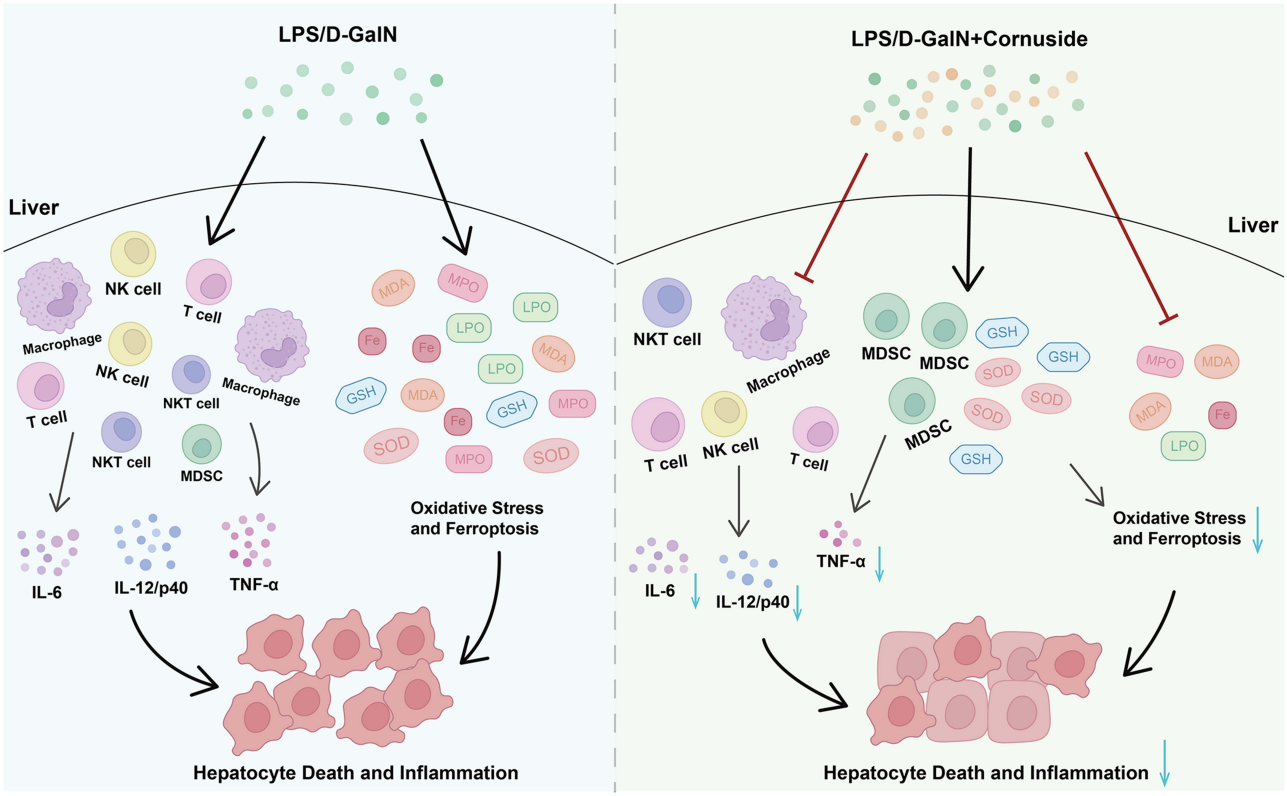

Figure 10 Mechanistic model for hepatoprotective effect of cornuside on LPS/D-GalN-induced ALF. The hepatoprotective effects of cornuside may be associated with suppressing excessive inflammatory responses, reducing oxidative stress, and modulating ferroptosis-associated ACSL4/xCT/Gpx4 signaling. "→" indicates promotion or positive regulation; "⊥" indicates inhibition or negative regulation.

Abbreviations

ALB, albumin; AKT1, AKT serine/threonine kinase 1; ALT, alanine aminotransferase; APAP, acetaminophen; AST, aspartate aminotransferase; BMDMs, bone marrow-derived macrophages; BSA, bovine serum albumin; CASP3, caspase-3; Con A, concanavalin A; DMEM, dulbecco's modified eagle medium; EGFR, epidermal growth factor receptor; ELISA, enzyme-linked immunosorbent assay; ESR1, estrogen receptor 1; GAPDH, glyceraldehyde 3-phosphate dehydrogenase; GM-CSF, granulocyte-macrophage colony stimulating factor; GO, Gene Ontology; GSH, glutathione; H&E, hematoxylin and eosin; HMNC, hepatic mononuclear cell; IFN, interferon; IGF1, insulin-like growth factor 1; IL, interleukin; iNOS, inducible nitric oxide synthase; JNK, c-Jun N-terminal kinase; KEGG, Kyoto Encyclopedia of Genes and Genomes; LPS, lipopolysaccharide; MAPK, mitogen-activated protein kinase; MDA, malondialdehyde; MIP-2, macrophage inflammatory protein 2; MPO, myeloperoxidase; NF, nuclear factor; NK, natural killer; NKT, natural killer T; Nrf2, nuclear factor erythroid 2-related factor 2; OMIM, online mendelian inheritance in man; PBS, phosphate buffered saline; PPARG, peroxisome proliferator-activated receptor gamma; PPI, protein–protein interaction; PSMF, phenylmethylsulfonyl fluoride; ROS, reactive oxygen species; qRT-PCR, Quantitative reverse transcription-polymerase chain reaction; RIPA, radio immunoprecipitation assay; SEM, standard error of the mean; SOD, superoxide dismutase; TNF-α, tumor necrosis factor-α; TUNEL, TdT-mediated dUTP Nick-End Labeling.

Data Sharing Statement

All data generated or analyzed during this study are available from the corresponding author Hui Zhang (Email: zhanghuitjwh@hotmail.com.) upon reasonable request.

Ethical Approval

All animal experiments were conducted in compliance with the Institutional Animal Welfare Guidelines and had been approved by the Animal Care and Use Committee of Jining Medical University (Approval No.: JNMC-2023-DW-131).

Acknowledgments

We thank Editage (https://www.editage.com) for English language editing.

Author Contributions

All authors made a significant contribution to the work reported, whether that is in the conception, study design, execution, acquisition of data, analysis and interpretation, or in all these areas; took part in drafting, revising or critically reviewing the article; gave final approval of the version to be published; have agreed on the journal to which the article has been submitted; and agree to be accountable for all aspects of the work.

Funding

This study was supported by National Natural Science Foundation of China (82171810), Natural Science Foundation of Shandong Province (ZR2025QC842, ZR2023QH332, ZR2021MH287), Research Fund for Academician Lin He New Medicine (JYHL2022MS21), Projects of Medical and Health Technology Development Program in Shandong Province (202202070388). Shandong Training Program of Innovation and Entrepreneurship for Undergraduates (No. S202510443043).

Disclosure

The authors report no conflicts of interest in this work.

References

1. Shingina A, Mukhtar N, Wakim-Fleming J. et al. Acute Liver Failure Guidelines. *Am J Gastroenterol*. 2023;118(7):1128–1153. doi:10.14309/ajg.0000000000002340
2. Wendon J, Cordoba J, Dhawan A, et al. EASL Clinical Practical Guidelines on the management of acute (fulminant) liver failure. *J Hepatol*. 2017;66(5):1047–1081. doi:10.1016/j.jhep.2016.12.003
3. He J, Feng X, Liu Y, et al. Graveoline attenuates D-GalN/LPS-induced acute liver injury via inhibition of JAK1/STAT3 signaling pathway. *Biomed Pharmacother*. 2024;177:117163. doi:10.1016/j.biopha.2024.117163
4. Ma W, Huo X, Li R, Xing J, Xu L, Yu D. piR-16404 drives ferroptotic liver injury via CASTOR1/mTORC1/GPX4 dysregulation in HepG2 cells and mice: a novel toxicity mechanism of N, N-dimethylformamide. *Arch Toxicol*. 2026;100(2):569–583. doi:10.1007/s00204-025-04198-7
5. Li WR, Li YK, Ren H, Guo Z, Xiao CL, Luo JQ. Lactobacillus reuteri attenuates methotrexate-induced liver injury via modulation of oxidative stress and inflammation through HO-1/GPX4 and NF-κB/NLRP3 pathways. *Eur J Pharmacol*. 2025;1006:178185. doi:10.1016/j.ejphar.2025.178185
6. Wu S, Zhao J, Fang X, Liao P, Liu G. From Toxicity Assessment to In Vivo Validation: exploring the Molecular Mechanisms of Triclosan-Induced Liver Injury. *Chem Res Toxicol*. 2026;39(1):117–129. doi:10.1021/acs.chemrestox.5c00380
7. Wang M, Chen F, Gao J, et al. Clusterin Drives Fiber Endocytosis by Mesothelial Cells to Resolve Liver Fibrosis. *Gastroenterology*. 2026;170(3):569–583. doi:10.1053/j.gastro.2025.08.022
8. Silverstein R. D-Galactosamine lethality model: scope and limitations. *J Endotoxin Res*. 2004;10(3):147–162. doi:10.1179/096805104225004879
9. Wang J, Luo J, Rotili D, et al. SIRT6 Protects Against Lipopolysaccharide-Induced Inflammation in Human Pulmonary Lung Microvascular Endothelial Cells. *Inflammation*. 2024;47(1):323–332. doi:10.1007/s10753-023-01911-5
10. Huang S, Wang Y, Xie S, et al. Hepatic TGFβr1 Deficiency Attenuates Lipopolysaccharide/D-Galactosamine–Induced Acute Liver Failure Through Inhibiting GSK3β–Nrf2–Mediated Hepatocyte Apoptosis and Ferroptosis. *CMGH*. 2022;13(6):1649–1672. doi:10.1016/j.jcmgh.2022.02.009
11. Tuñón MJ, Alvarez M, Culebras JM, González-Gallego J. An overview of animal models for investigating the pathogenesis and therapeutic strategies in acute hepatic failure. *WJG*. 2009;15(25):3086. doi:10.3748/wjg.15.3086
12. Wu J, Wang Y, Jiang R, et al. Ferroptosis in liver disease: new insights into disease mechanisms. *Cell Death Discov*. 2021;7(1):276. doi:10.1038/s41420-021-00660-4
13. Wang S, Ma D, Yang M, Zhang Y, Wang S, Zhou W. Arsenic trioxide-based nanoparticles for enhanced chemotherapy by activating pyroptosis. *Acta Pharmaceutica Sinica B*. 2025;15(11):6001–6018. doi:10.1016/j.apsb.2025.08.003
14. Bloomer SA, Brown KE. Hepcidin and Iron Metabolism in Experimental Liver Injury. *Am J Pathol*. 2021;191(7):1165–1179. doi:10.1016/j.ajpath.2021.04.005
15. He J, Du C, Li C, et al. Ferroptosis in acute liver Failure: unraveling the hepcidin-ferroportin axis and therapeutic interventions. *Redox Biol*. 2025;84:103657. doi:10.1016/j.redox.2025.103657
16. Ong SY, Gurrin LC, Dolling L, et al. Reduction of body iron in HFE -related haemochromatosis and moderate iron overload (Mi-Iron): a multicentre, participant-blinded, randomised controlled trial. *Lancet Haematol*. 2017;4(12):e607–e614. doi:10.1016/S2352-3026(17)30214-4
17. Liu CY, Wang M, Yu HM, et al. Ferroptosis is involved in alcohol-induced cell death *in vivo* and *in vitro*. *Biosci Biotechnol Biochem*. 2020;84(8):1621–1628. doi:10.1080/09168451.2020.1763155
18. Gao G, Xie Z, wen LE, et al. Dehydroabietic acid improves nonalcoholic fatty liver disease through activating the Keap1/Nrf2-ARE signaling pathway to reduce ferroptosis. *J Nat Med*. 2021;75(3):540–552. doi:10.1007/s11418-021-01491-4
19. Sun XJ, Xu GL. Overexpression of Acyl-CoA Ligase 4 (ACSL4) in Patients with Hepatocellular Carcinoma and its Prognosis. *Med Sci Monit*. 2017;23:4343–4350. doi:10.12659/MSM.906639

20. Feng J, zhi LP, zhi ZG, et al. ACSL4 is a predictive biomarker of sorafenib sensitivity in hepatocellular carcinoma. *Acta Pharmacol Sin*. 2021;42 (1):160–170. doi:10.1038/s41401-020-0439-x
21. Zeng Y, He Y, Wang L, et al. Dihydroquercetin improves experimental acute liver failure by targeting ferroptosis and mitochondria-mediated apoptosis through the SIRT1/p53 axis. *Phytomedicine*. 2024;128:155533. doi:10.1016/j.phymed.2024.155533
22. Li QY, Dou ZM, Chen C, Jiang YM, Yang B, Fu X. Study on the Effect of Molecular Weight on the Gut Microbiota Fermentation Properties of Blackberry Polysaccharides In Vitro. *J Agric Food Chem*. 2022;70(36):11245–11257. doi:10.1021/acs.jafc.2c03091
23. Chen X, Chen C, Ma C, Kang W, Wu J, Fu X. *Dendrobium officinale* polysaccharide attenuates type 2 diabetes in mice model by modulating gut microbiota and alleviating intestinal mucosal barrier damage. *Food Science and Human Wellness*. 2025;14(1):9250007. doi:10.26599/FSHW.2024.9250007
24. Huang J, Zhang Y, Dong L, et al. Ethnopharmacology, phytochemistry, and pharmacology of Cornus officinalis Sieb. et Zucc. *J Ethnopharmacol*. 2018;213:280–301. doi:10.1016/j.jep.2017.11.010
25. Zhang R, Liu J, Xu B, Wu Y, Liang S, Yuan Q. Cornuside alleviates experimental autoimmune encephalomyelitis by inhibiting Th17 cell infiltration into the central nervous system. *J Zhejiang Univ Sci B*. 2021;22(5):421–430. doi:10.1631/jzus.B2000771
26. Song SZ, Choi YH, Jin GY, Li GZ, Yan GH. Protective Effect of Cornuside against Carbon Tetrachloride-Induced Acute Hepatic Injury. *Biosci Biotechnol Biochem*. 2011;75(4):656–661. doi:10.1271/bbb.100739
27. Quah Y, Lee SJ, Lee EB, et al. Cornus officinalis Ethanolic Extract with Potential Anti-Allergic, Anti-Inflammatory, and Antioxidant Activities. *Nutrients*. 2020;12(11):3317. doi:10.3390/nu12113317
28. Ryu SH, Kim C, Kim N, Lee W, Bae JS. Inhibitory functions of cornuside on TGFBIp-mediated septic responses. *J Nat Med*. 2022;76(2):451–461. doi:10.1007/s11418-021-01601-2
29. Wang L, Yan F, Zhang J, et al. Cornuside improves murine autoimmune hepatitis through inhibition of inflammatory responses. *Phytomedicine*. 2023;120:155077. doi:10.1016/j.phymed.2023.155077
30. Knox C, Wilson M, Klinger CM, et al. DrugBank 6.0: the DrugBank Knowledgebase for 2024. *Nucleic Acids Res*. 2024;52(D1):D1265–D1275. doi:10.1093/nar/gkad976
31. Zhou Y, Zhang Y, Zhao D, et al. TTD: *therapeutic Target Database* describing target druggability information. *Nucleic Acids Res*. 2024;52(D1): D1465–D1477. doi:10.1093/nar/gkad751
32. Piñero J, Ramírez-Anguita JM, Saüch-Pitarch J, et al. The DisGeNET knowledge platform for disease genomics: 2019 update. *Nucleic Acids Res*. 2019;2019:gkz1021. doi:10.1093/nar/gkz1021
33. Fischer AH, Jacobson KA, Rose J, Zeller R. Hematoxylin and Eosin Staining of Tissue and Cell Sections. *Cold Spring Harb Protoc*. 2008;2008 (5):4986. doi:10.1101/pdb.prot4986
34. Harrill AH, Roach J, Fier I, et al. The Effects of Heparins on the Liver: application of Mechanistic Serum Biomarkers in a Randomized Study in Healthy Volunteers. *Clin Pharmacol Ther*. 2012;92(2):214–220. doi:10.1038/clpt.2012.40
35. Maiwall R, Kulkarni AV, Arab JP, Piano S. Acute liver failure. *Lancet*. 2024;404(10454):789–802. doi:10.1016/S0140-6736(24)00693-7
36. Zhang H, Gao M, Wang H, et al. Atractylenolide I prevents acute liver failure in mouse by regulating M1 macrophage polarization. *Sci Rep*. 2025;15(1):4015. doi:10.1038/s41598-025-86977-x
37. Ruart M, Chavarria L, Campreciós G, et al. Impaired endothelial autophagy promotes liver fibrosis by aggravating the oxidative stress response during acute liver injury. *J Hepatol*. 2019;70(3):458–469. doi:10.1016/j.jhep.2018.10.015
38. Allameh A, Niayesh-Mehr R, Aliarab A, Sebastiani G, Pantopoulos K. Oxidative Stress in Liver Pathophysiology and Disease. *Antioxidants*. 2023;12(9):1653. doi:10.3390/antiox12091653
39. Gong C, Fu X, Ma Q, et al. Gastrodin: modulating the xCT/GPX4 and ACSL4/LPCAT3 pathways to inhibit ferroptosis after ischemic stroke. *Phytomedicine*. 2025;136:156331. doi:10.1016/j.phymed.2024.156331
40. Du WJ, Liu L, Sun C, Yu JH, Xiao D, Li Q. Prodromal fever indicates a high risk of liver failure in acute hepatitis B. *Inter J Infect Dis*. 2017;57:98–103. doi:10.1016/j.ijid.2017.02.009
41. Zhang A, Sun H, Wang X. Recent advances in natural products from plants for treatment of liver diseases. *Eur J Med Chem*. 2013;63:570–577. doi:10.1016/j.ejmech.2012.12.062
42. Li X, Ge J, Zheng Q, Zhang J, Sun R, Liu R. Evodiamine and rutaecarpine from Tetradium ruticarpum in the treatment of liver diseases. *Phytomedicine*. 2020;68:153180. doi:10.1016/j.phymed.2020.153180
43. Liu Z, Yan F, Zhang H, et al. Zingerone attenuates concanavalin A-induced acute liver injury by restricting inflammatory responses. *Int Immunopharmacol*. 2024;142:113198. doi:10.1016/j.intimp.2024.113198
44. Liu Z, Gao M, Yan F, et al. Cucurbitacin IIb mitigates concanavalin A-induced acute liver injury by suppressing M1 macrophage polarization. *Int Immunopharmacol*. 2025;147:113964. doi:10.1016/j.intimp.2024.113964
45. Tang L, Wang F, Xiao L, et al. Yi-Qi-Jian-Pi formula modulates the PI3K/AKT signaling pathway to attenuate acute-on-chronic liver failure by suppressing hypoxic injury and apoptosis in vivo and in vitro. *J Ethnopharmacol*. 2021;280:114411. doi:10.1016/j.jep.2021.114411
46. Jiang Z, Yang X, Han Y, et al. Sarmentosin promotes USP17 and regulates Nrf2-mediated mitophagy and cellular oxidative stress to alleviate APAP-induced acute liver failure. *Phytomedicine*. 2022;104:154337. doi:10.1016/j.phymed.2022.154337
47. Zigmond E, Samia-Grinberg S, Pasmanik-Chor M, et al. Infiltrating Monocyte-Derived Macrophages and Resident Kupffer Cells Display Different Ontogeny and Functions in Acute Liver Injury. *J Immunol*. 2014;193(1):344–353. doi:10.4049/jimmunol.1400574
48. Wei L, Ren F, Zhang X, et al. Oxidative stress promotes d-GalN/LPS-induced acute hepatotoxicity by increasing glycogen synthase kinase 3β activity. *Inflamm Res*. 2014;63(6):485–494. doi:10.1007/s00011-014-0720-x
49. Chen J, Li X, Ge C, Min J, Wang F. The multifaceted role of ferroptosis in liver disease. *Cell Death Differ*. 2022;29(3):467–480. doi:10.1038/s41418-022-00941-0
50. Dixon SJ, Olzmann JA. The cell biology of ferroptosis. *Nat Rev Mol Cell Biol*. 2024;25(6):424–442. doi:10.1038/s41580-024-00703-5
51. Chen X, Kang R, Kroemer G, Tang D. Ferroptosis in infection, inflammation, and immunity. *J Exp Med*. 2021;218(6). doi:10.1084/jem.20210518
52. Ursini F, Maiorino M. Lipid peroxidation and ferroptosis: the role of GSH and GPx4. *Free Radic Biol Med*. 2020;152:175–185. doi:10.1016/j.freeradbiomed.2020.02.027